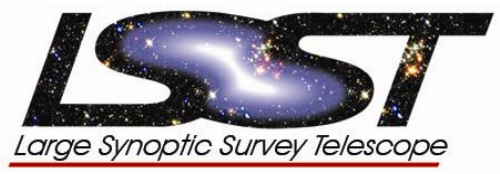

Content Controlled Document

Handle: LSE-40

Release Status: Unrestricted - Public Release

The LSST Photon Rates and SNR Calculations, v1.2

Author(s): Zeljko Ivezic, Lynne Jones, and Robert Lupton

Date: May 1, 2010

Summary: Addresses questions concerning photon rate, dark sky photon rate, signal to noise, required system throughput

Certification Details
This LSST document was approved on the date shown below as a Content-Controlled Document by the LSST Change Control Board. If this document is changed or superseded the new document will retain the Handle designation shown above. The control is on the most recent digital document with this Handle in the LSST digital archive and not printed versions. Additional information may be found in the LSST CCB minutes.

Date of CCB Action: May 13, 2010

Change Log

Handle: **LSE-40**

Date: **May 1, 2010**

Title: **The LSST Photon Rates and SNR Calculations, v1.2**

Authors: **Zeljko Ivezic, Lynne Jones, and Robert Lupton**

Revision Author(s)	Revision Date	Description of Revisions
Rev Authors	Click to enter date.	Click here to enter text.
Rev Authors	Click to enter a date.	Click here to enter text.
Rev Authors	Click here to enter a date.	Click here to enter text.
Rev Authors	Click here to enter a date.	Click here to enter text.
Rev Authors	Click here to enter a date.	Click here to enter text.
Rev Authors	Click here to enter a date.	Click here to enter text.
Rev Authors	Click here to enter a date.	Click here to enter text.
Rev Authors	Click here to enter a date.	Click here to enter text.
Rev Authors	Click here to enter a date.	Click here to enter text.

The LSST Photon Rates and SNR Calculations, v1.2

Željko Ivezić, Lynne Jones, and Robert Lupton, May 1, 2010

ABSTRACT

This document discusses the following questions in the context of the LSST: 1) Given the AB magnitude of a source and the shape of its spectral energy distribution, what is its photon rate per m^2 and second in a specified bandpass? 2) What is the photon rate for a standard dark sky?, 3) Given instrumental properties and observing conditions such as the seeing and atmospheric transmissivity, what is the attained signal-to-noise ratio for a given source?, and 4) Given the SRD single-visit limiting depths, what is the minimum system throughput needed to attain them? We also describe python code for computing these quantities for a standardized set of conditions, and provide instructions for its retrieval.

1. Introduction

This document and supporting python code make the SNR calculation (and resulting system throughput requirements, such as detector quantum efficiency) standardized and easily reproducible across the LSST project. The calculation of the signal-to-noise ratio (SNR) for a source detection involves predicting its ADU counts and accounting for all noise contributions. A similar calculation is implemented in the LSST Exposure Time Calculator developed for the LSST by Gee et al. (ETC[1]). ETC provides a user-friendly interface and can perform this calculation for different source brightness and spectral energy distributions, and for a variety of observing conditions (including bright time). While similar in spirit to ETC calculations, the main purpose of this document is to provide an easy-to-follow transparent semi-analytic description of these calculations for the case of a standard source, fiducial observing conditions and *version-controlled* instrument properties.

We begin by discussing expected count rate from an arbitrary source, followed by a section on standardized sky emission spectrum. The signal-to-noise ratio calculation is discussed in Section 4, and its application to a proposed standardized case is described in Section 5. The main result, generalized standardized SRD-based constraints on the system throughput, are discussed in Section 6.

[1]See http://dls.physics.ucdavis.edu/etc/

2. From Photons to Counts

Given $F_\nu(\lambda)$, the specific flux[2] of an object *at the top* of the atmosphere, the flux transmitted through the atmosphere to the telescope pupil is

$$F_\nu^{pupil}(\lambda) = F_\nu(\lambda)\, S^{atm}(\lambda), \tag{1}$$

where $S^{atm}(\lambda)$ is the (dimensionless) probability that a source photon of wavelength λ makes it through the atmosphere,

$$S^{atm}(\lambda) = \mathrm{e}^{-\tau^{atm}(\lambda)}. \tag{2}$$

Here $\tau^{atm}(\lambda)$ is the optical depth of the atmospheric layer at wavelength λ towards the source (clouds represent an additive contribution to τ^{atm}). While both $F_\nu(\lambda)$ and $\tau^{atm}(\lambda)$ can be functions of time, it is assumed hereafter that all quantities are averaged over some short (exposure) time.

Given $F_\nu^{pupil}(\lambda)$, the recorded ADU counts in a band b can be written as

$$C_b = C \int_0^\infty F_\nu^{pupil}(\lambda)\, S_b^{sys}(\lambda)\lambda^{-1} d\lambda. \tag{3}$$

Here, $S_b^{sys}(\lambda)$ is the (dimensionless) probability that a photon that hits the telescope pupil will be converted into an ADU count, and the term λ^{-1} comes from the conversion of energy per unit frequency into the number of photons per unit wavelength ($b = ugrizy$). The dimensional conversion constant C is

$$C = \frac{\pi D^2 \Delta t}{4gh} \tag{4}$$

where D is the effective primary mirror diameter, Δt is the exposure time, g is the gain of the readout electronics (number of photo-electrons per ADU count, a number greater than one that should really be called inverse gain), and h is the Planck constant.

The system response function, $S_b^{sys}(\lambda)$, includes the multiplicative effects of the mirror reflectances, transmission of the lenses and filters, and quantum efficiency of the camera sensors.

$$S^{sys}(\lambda) = S^{\mathrm{mirrors}}(\lambda)\, S^{\mathrm{lenses}}(\lambda)\, S^{\mathrm{filter}}(\lambda)\, S^{\mathrm{detector}}(\lambda) \tag{5}$$

where all listed functions are dimensionless probability functions. The adopted baseline system throughput is shown in Fig. 1 and available from the LSST Docushare Collection-1777.

For a source with spectral energy distribution $F_\nu(\lambda) = F_o f_\nu(\lambda)$, the corresponding number of ADU (not photo-electrons, note division by gain g) is

$$C_b = \frac{5,455}{g} 10^{0.4(25-m_{AB})} \left(\frac{D}{6.5\mathrm{m}}\right)^2 \left(\frac{\Delta t}{30\,\mathrm{sec}}\right) \int_0^\infty f_\nu(\lambda)\, S^{atm}(\lambda)\, S_b^{sys}(\lambda)\lambda^{-1} d\lambda. \tag{6}$$

[2]Hereafter, the units for specific flux are Jansky (1 Jy = 10^{-26} W Hz^{-1} m^{-2} = 10^{-23} erg cm^{-2}s^{-1} Hz^{-1}). The choice of F_ν vs. F_λ, for example, makes the flux conversion to AB magnitude scale more transparent. The choice of wavelength for the running variable is more convenient than the choice of frequency.

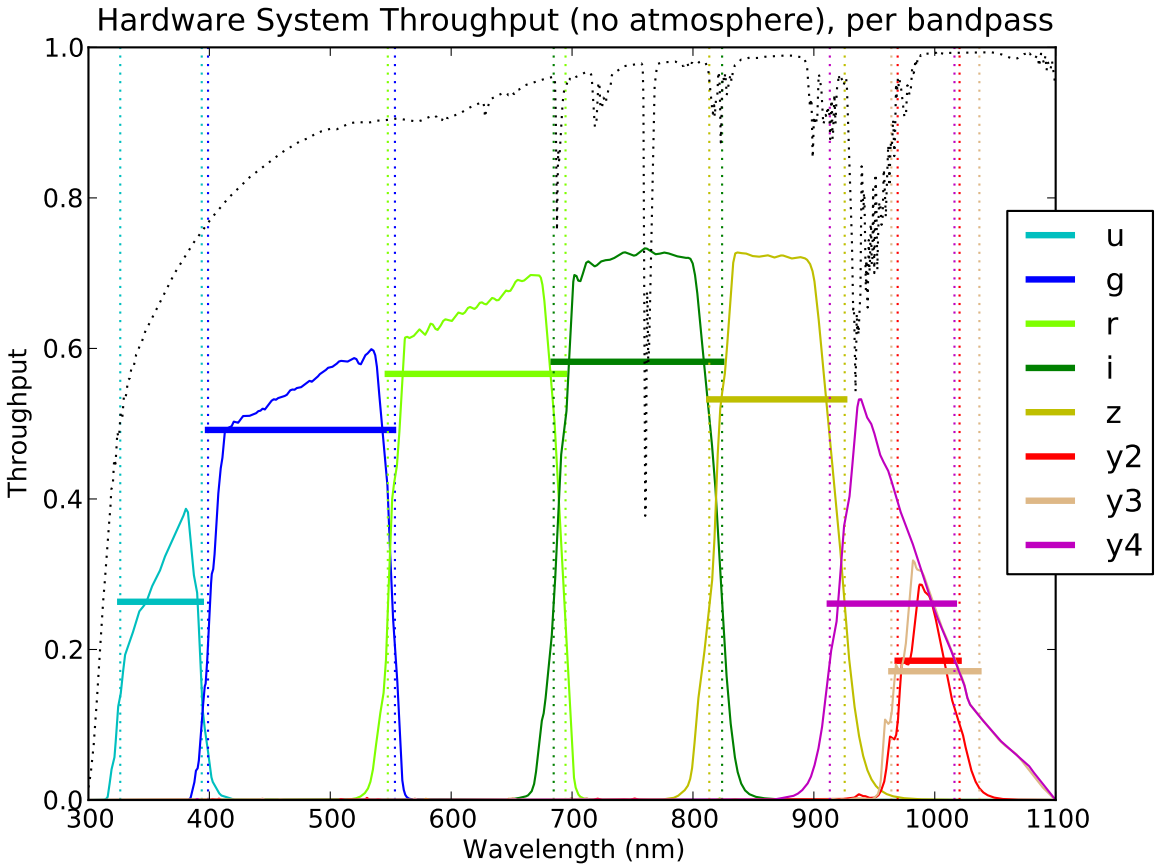

Fig. 1.— The adopted system throughput (without atmosphere!) for each band is shown by colored lines, according to the legend. The data files, consecutively numbered from Document-8846 to Document-8853 are available from Collection-1777. The horizontal lines are "characteristic" bandpass throughput defined in Section 5. The black dotted line shows atmospheric transmissivity at airmass $X = 1$ from Fig. 2. The vertical dotted lines mark wavelengths where the system throughput in each band drops to a fiducial value of 35% of its peak value.

where $m_o = -2.5 \log_{10}(F_o/3631\mathrm{Jy})$ is the AB magnitude corresponding to flux F_o (note that $f_\nu(\lambda)$ is dimensionless by definition). The numerical values of this integral are discussed for a standardized case in Section 5.

The extracted counts for any source depend on the applied count weighting scheme across the pixels. In the context of signal-to-noise calculation discussed here, only point sources with optimally extracted counts are considered (see Section 4).

3. The Standard Atmosphere and Standard Sky Spectrum

In this Section, we describe the adopted standard atmosphere and standard sky spectrum. These two quantities play important roles when translating the limiting depth requirements from the SRD into constraints on the overall system throughput, $S_b^{sys}(\lambda)$.

3.1. The Standard Atmosphere

The standard 1976 U.S. Atmosphere computed using the MODTRAN4 code at airmass $X = 1$ is adopted for the SNR calculations. The atmospheric transmittance is computed from space to Pachon at 2.7 km elevation above sea level. The code computes the molecular scattering and molecular absorption by water vapor, ozone, and the mixture of oxygen and other trace elements. The resulting transmission curve is available as Document-8817 and is shown in Figure 2.

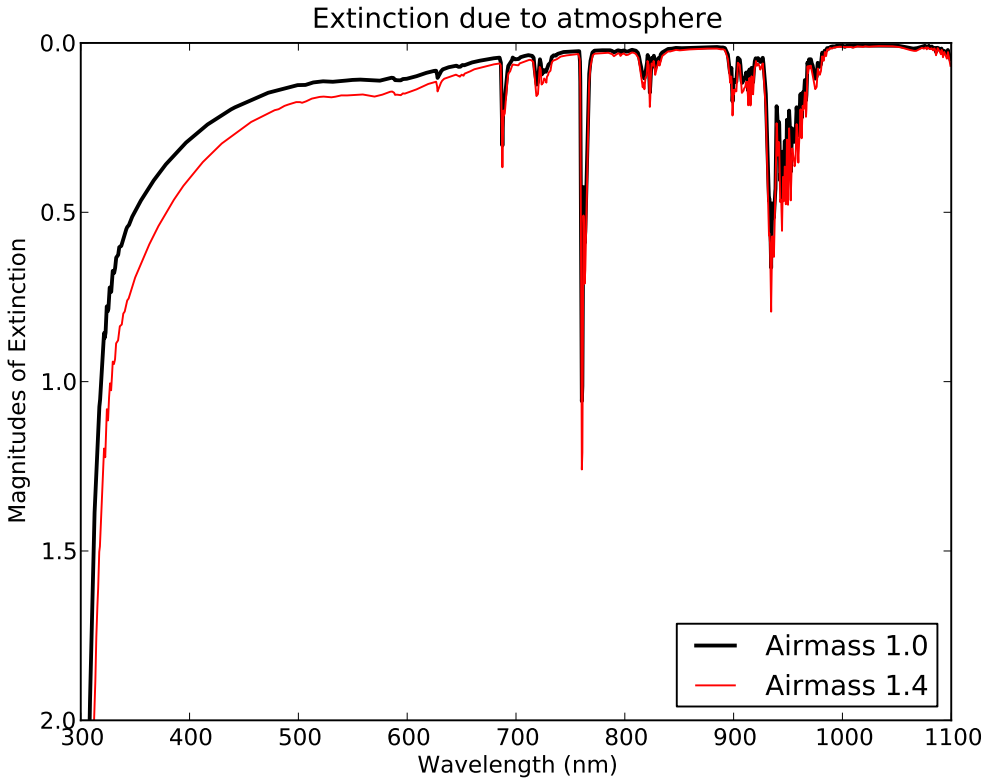

Fig. 2.— The extinction (mag) for the adopted standard atmosphere at airmass $X = 1$ (black curve). For comparison, atmospheric extinction at $X = 1.4$ is also shown (red curve). Both curves were generated using the MODTRAN4 code with standard input parameters, and are available as Document-8817.

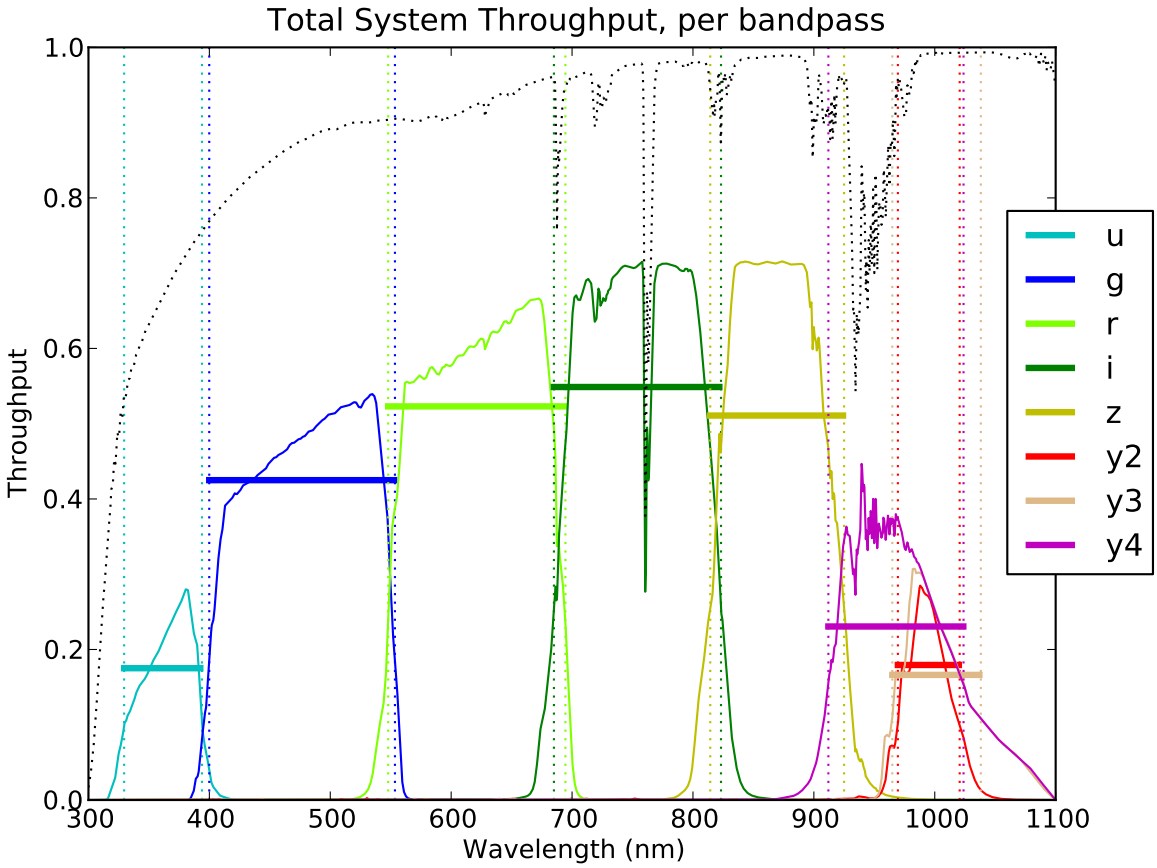

Fig. 3.— The adopted total throughput (atmosphere and system, see eq. 7) for each band is shown by colored lines, according to the legend. The horizontal lines are "characteristic" bandpass throughputs defined in Section 5. The black dotted line shows the atmospheric transmissivity at airmass $X = 1$ from Fig. 2. The vertical dotted lines mark wavelengths where the total throughput in each band drops to 35% of its peak value. The effects of optics, detectors and atmosphere on total throughput are shown separately in Fig. 6 in Appendix A.

The baseline total throughput, defined as

$$S_b^{tot}(\lambda) = S^{atm}(\lambda)\, S_b^{sys}(\lambda), \tag{7}$$

is shown in Fig. 3. The data files with $S_b^{tot}(\lambda)$ are consecutively numbered from Document-8835 to Document-8842, and are available from Collection-1777.

3.2. The Standard Sky Spectrum

The adopted dark sky spectrum at airmass $X = 1$ is based on several observed spectra (the UVES and Gemini near-IR data obtained from Perry Gee, and the "ESO" sky from Ferdinando

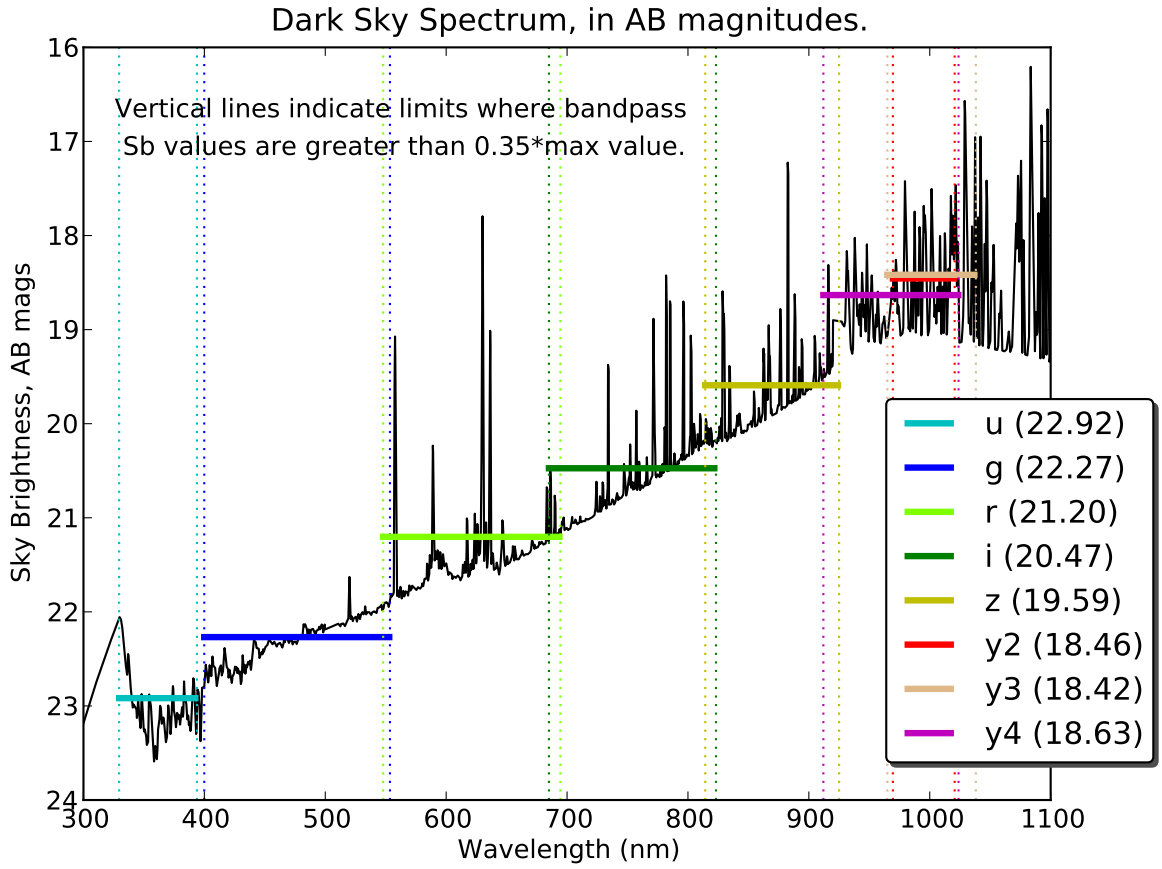

Fig. 4.— The adopted dark sky spectrum (black line), expressed in AB mag/arcsec^2. The horizontal lines are computed using the the baseline system response (see Fig. 3), via eq. 8. The data file is available as Document-8818.

Patat). They agree in the overlapping wavelength region but fail to reproduce the median SDSS dark sky brightness measurements. In order to rectify this discrepancy, the blue and red edges are multiplied by a low-order polynomial (for more details see the upcoming document on the LSST sky model, Jones et al., in prep.).

The adopted sky spectrum (Fig. 4) reproduces the median SDSS dark sky magnitudes when convolved with SDSS system bandpasses, and is available as Document-8818. Observed and synthesized SDSS sky brightness are listed in Table 1, together with the sky brightness synthesized using the baseline LSST bandpasses as

$$m_b^{sky} = -2.5 \log_{10} \left(\frac{\int_0^\infty b_\nu^{sky}(\lambda)\, S_b^{sys}(\lambda) \lambda^{-1} d\lambda}{3631\,\mathrm{Jy} \int_0^\infty S_b^{sys}(\lambda) \lambda^{-1} d\lambda} \right), \quad (8)$$

where $b_\nu^{sky}(\lambda)$ is the adopted sky spectrum in Jy/arcsec^2 (the angular units appear not to cancel out in this expression; of course, arcsec is dimensionless, but it needs to be remembered that the

Quantity	u	g	r	i	z	y_2	y_3	y_4
Observed SDSS sky	22.88	22.29	21.22	20.46	19.23	–	–	–
Synthesized SDSS sky	22.83	22.33	21.18	20.52	19.25	–	–	–
LSST baseline dark sky	22.92	22.27	21.20	20.47	19.59	18.46	18.42	18.63

Table 1: The sky surface brightness for the sky spectrum shown in Fig. 4 (and available as Document-8818). The first row lists the median measured SDSS dark time sky brightness compiled by Perry Gee (AB magnitudes per arcsec^2, uncorrected for atmospheric extinction). The second row lists sky brightness synthesized using the standardized sky emission spectrum and SDSS bandpasses. The third row lists LSST sky brightness (AB magnitudes per arcsec^2) synthesized using the standardized sky emission spectrum and LSST baseline system response (see Fig. 3), via eq. 8.

adopted surface brightness definition is based on arcsec and not on, e.g., radian). Note that the sky brightness computation does **not** include $S^{atm}(\lambda)$ because the sky spectrum is **defined** to correspond to the telescope pupil (and measured as such by SDSS[3]). The baseline system response used in this calculation is shown in Fig. 1.

4. The Computation of the Signal-to-Noise Ratio

A source which delivered a total of C_o^T counts in an image is detected on top of a flat background (C_o^T corresponds to count rate given by eq. 3, but is not identical to C_b due to counting statistics; for large C_b, C_o^T follows a Gaussian distribution centered on C_b, with an rms of $\sqrt{C_b/g}$; see eq. 41). This section describes how to compute the noise, N_o, associated with various methods for measuring C_o, an estimator for C_o^T. The resulting signal-to-noise ratio, $SNR = C_o/N_o$, is required to translate the SRD specifications for limiting 5σ magnitudes (Table 6, SRD v4.3.3) into overall system throughput. Due to non-vanishing background and finite width of the source image, optimal estimation of C_o^T, i.e. the determination of C_o, is not as simple as it may appear at first (e.g., "Just add up the counts...").

4.1. Basic SNR Considerations

The source signal (counts) in pixel i, C_i, is the difference between the observed photon flux, O_i, and the background photon flux, B,

$$C_i = O_i - B. \tag{9}$$

The background photon flux (typically dominated by sky emission) is assumed constant over the pixels subtended by the source, and measured with an error σ_B (this is not the Poissonian fluctuation

[3]When SDSS sky brightness is downloaded as a photometrically calibrated SDSS data product, the values are inappropriately corrected for atmospheric extinction. This correction was "uncorrected" in the median SDSS sky values collated by P.Gee and used here (see Table 1).

of B but rather the error in the determination of the mean background level; e.g., optical sky has substantial spatial structure at red wavelengths). Both B and σ_B are expressed in counts per pixel per readout.

An estimator for the total number of counts associated with the source can be written as

$$C_o = \sum_i w_i C_i, \tag{10}$$

where w_i are appropriately chosen weights summed over pixels, and discussed in more detail below. It is **not** required that $\sum_i w_i = 1$.

The noise associated with this measurement of C_o includes the correspondingly weighted noise in the determination of O_i and the instrumental noise, σ_{inst} (dominated by read-out noise and dark current, but more generally can include all other noise that is independent of the signal strength), which can be added in quadrature

$$N_o^2 = C_o/g + (B/g + \sigma_B^2 + \sigma_{inst}^2) \sum_i w_i. \tag{11}$$

Here g is the instrument gain (the number of photo-electrons per ADU, typically larger than 1), and enters because counting (Poissonian) statistics applies to photo-electrons rather than to ADU.

As evident, the resulting SNR crucially depends on the applied weights. Introducing a more compact form, $\sigma_{tot}^2 = (B/g + \sigma_B^2 + \sigma_{inst}^2)$,

$$N_o^2 = C_o/g + \sigma_{tot}^2 \sum_i w_i. \tag{12}$$

For *qualitative* comparison of different aperture weighting schemes, we introduce an approximation valid in the weak-signal limit (sometimes called background-dominated case, but note that σ_{inst} need not be negligible) with $C_o/g \ll \sigma_{tot}^2 \sum_i w_i$,

$$SNR_B = \frac{C_o}{\sigma_{tot}} \left(\sum_i w_i \right)^{-1/2}. \tag{13}$$

This is good approximation at the faint end (SNR$\sim$5) in all bands except for the u band.

Below we address two most popular count extraction methods that produce the so-called aperture and point-spread-function (psf) counts. In order to compare their performance, an image profile has to be assumed. For pedagogical reasons, we first assume a simple Gaussian profile

$$p(r|\alpha) = \frac{1}{2\pi\alpha^2} \exp\left(-\frac{r^2}{2\alpha^2}\right), \tag{14}$$

which satisfies $2\pi \int_0^\infty p(r|\alpha) r dr = 1$, and FWHM=$2.355\alpha$. The source is then described by

$$C(r) = C_o^T \, p(r|\alpha). \tag{15}$$

The final SNR calculation utilizes a more complicated profile consistent with the SRD and discussed in Section 4.4.

4.2. Aperture Counts

Aperture counts are often used as an estimator of C_o^T with weights $w_i = 1$ for $r \leq r_{aper}$ and $w_i = 0$ for $r > r_{aper}$, where r_{aper} is the aperture radius. The total number of pixels inside the aperture is

$$N_{pix} = \sum_i w_i = \pi(r_{aper}/\mathrm{pixelScale})^2, \tag{16}$$

where pixelScale is the pixel angular size (arcsec/pixel). For the background-dominated case,

$$SNR_B = \frac{C_o}{\sigma_{tot} N_{pix}^{1/2}}. \tag{17}$$

Unless r_{aper} is infinite, C_o is a **biased** estimator of C_o^T ($C_o < C_o^T$); for the adopted Gaussian profile (eq. 14),

$$C_o(r_{aper}) = C_o^T \left[1 - \exp\left(-\frac{r_{aper}^2}{2\alpha^2}\right)\right]. \tag{18}$$

While this bias can be corrected when the image profile is perfectly known, decreased SNR due to smaller source counts cannot be avoided. However, r_{aper} cannot be too large because of the background contribution to noise, which increases proportionally to r_{aper}^2 (eq. 11). By maximizing the SNR as a function of r_{aper}, it is straightforward to show that the SNR is maximized for $r_{aper} = 1.585\alpha$, corresponding to an aperture diameter of 1.346*FWHM, where FWHM is the seeing (FWHM=2.355α for gaussian profile). The optimal number of pixels for extracting aperture counts is thus

$$N_{pix}^{aper} = 1.42\,(\mathrm{FWHM}/\mathrm{pixelScale})^2. \tag{19}$$

In this case, the aperture includes 71.5% of the total source flux, which in the background-limited case (i.e. when the source contribution to noise in eq. 11 is negligible) corresponds to

$$SNR_B^{aper,max} = \frac{C_o^T}{\sigma_{tot}} \frac{0.60}{(\mathrm{FWHM}/\mathrm{pixelScale})}. \tag{20}$$

This maximum attainable SNR for a top-hat extraction profile is equal to 90% of the optimal SNR based on the psf profile (see below), and thus the difference between aperture and psf count extraction errors may at first appear to be negligible. However, since aperture counts extracted with $r_{aper} = 1.346$FWHM include only 71.5% of the total source flux, they are extremely sensitive to errors in seeing determination, and to seeing variations when r_{aper} is kept fixed (~ 0.1 mag flux difference for a 10% seeing variation). When r_{aper} is doubled to include 99% of the total flux, the SNR decreases by 44% (to alleviate such a loss of SNR, the exposure time would have to be doubled). The sensitivity of aperture flux computed with a fixed r_{aper} to seeing variations is mitigated by using a maximum likelihood estimator to extract total source counts.

4.3. Optimally Extracted Counts

The optimal estimate of C_o^T for an unresolved source is based on

$$w_i = \frac{p_i}{\sum_i p_i^2}, \tag{21}$$

where p_i are the values of the point spread function (psf) profile in each pixel ($\sum_i p_i = 1$). This expression comes from maximum likelihood considerations. If the psf profile is known, the determination of the amplitude C_o^T (see eq. 15) is equivalent to fitting this *known* profile to the observed source profile. The log(likelihood) for this fit is given by

$$L(C_o) = \text{const.} - \frac{1}{2}\sum_i \frac{(C_i - C_o p_i)^2}{\sigma_i^2}, \tag{22}$$

where σ_i is the noise associated with each C_i measurement. The most likely value of C_o is found by maximizing $L(C_o)$, $dL/dC_o = 0$, and its associated error from $\sigma_C = (d^2L/dC_o^2)^{-1/2}$.

At the faint end $\sigma_i \sim \sigma_{tot} = \text{const.}$ (because the sky is the dominant noise contributor; c.f. eq. 11), and thus

$$L(C_o) = \text{const.} - \frac{1}{2\sigma_{tot}^2}\sum_i (C_i - C_o p_i)^2. \tag{23}$$

Hence,

$$C_o^{psf} = \frac{\sum_i p_i C_i}{\sum_i p_i^2}, \tag{24}$$

and

$$\sigma_C = \left(\frac{\sigma_{tot}^2}{\sum_i p_i^2}\right)^{1/2}. \tag{25}$$

It is important to note that C_o^{psf} is an **unbiased** estimator of C_o^T, and that σ_C is the **minimum possible** error for estimating C_o^T (in the context of SNR determination discussed here, several additional sources of small errors, such as the impact of centroiding errors, are neglected).

In analogy with aperture counts, it is customary to introduce the effective number of pixels,

$$n_{\rm eff} = \sum_i w_i = \frac{1}{\sum_i p_i^2}, \tag{26}$$

which for a single gaussian profile yields

$$n_{\rm eff} = 4\pi(\alpha/\text{pixelScale})^2 = 2.266\,(\text{FWHM/pixelScale})^2. \tag{27}$$

Note that eq. 26 can be used to easily estimate SNR for an arbitrary psf profile. Given $n_{\rm eff}$, the noise for optimal count extraction can be computed from

$$N_o^2 = C_o^T/g + \sigma_{tot}^2\, n_{\rm eff}. \tag{28}$$

In the limit $C_o^T/g \ll \sigma_{tot}^2 n_{\rm eff}$,

$$SNR_B^{psf} = \frac{C_o^T}{\sigma_{tot}}\frac{0.66}{(\text{FWHM/pixelScale})}, \tag{29}$$

which is 10% higher than for the best-case aperture count extraction (the background noise is 26% larger in the optimal case, but there is no loss of source counts). Therefore, *the estimated survey limiting depth is about 0.1 mag deeper when assuming optimal count extraction.*

4.4. The Seeing Profile Expected for Kolmogorov turbulence

Until now, the source profile (point spread function) was assumed to be a single gaussian (see eq. 15). In this section we discuss a slightly more involved profile which is in much better agreement with the data and has theoretical foundation. This is the same profile as discussed in the SRD.

A good description of both typically-observed seeing profiles and those expected for Kolmogorov turbulence is a double-Gaussian profile

$$p_K(r|\alpha) = 0.909\,[p(r|\alpha) + 0.1p(r|2\alpha)] \tag{30}$$

where $p(r|\alpha)$ is given by eq. 14, and the coefficient 0.909 comes from the normalization requirement $2\pi\int_0^\infty p_K(r|\alpha)rdr = 1$.

Using eq. 26, for $p_K(r|\alpha)$

$$n_{\rm eff} = 2.436\,({\rm FWHM/pixelScale})^2 \tag{31}$$

or about 7.5% larger than for the case of a single Gaussian profile with the same FWHM. Therefore, for the profile assumed in the SRD and for optimal count extraction, in the background dominated case

$$SNR_B^{SRD} = \frac{C_o^T}{\sigma_{tot}}\frac{0.64}{({\rm FWHM/pixelScale})}. \tag{32}$$

Seeing is typically expressed using FWHM, but the SRD uses a generalized definition determined from the effective number of pixels, $n_{\rm eff}$,

$${\rm seeing} = 0.663\,{\rm pixelScale}\,\sqrt{n_{\rm eff}}\ {\rm arcsec}. \tag{33}$$

In the case of single Gaussian profile, the seeing computed from this expression is identical to FWHM. For the profile given by eq. 30, the seeing computed from eq. 33 is 1.035 times larger than FWHM, which is sufficiently small difference to be ignored in this context.

5. Standardized SNR Calculation

A source with flat spectral energy distribution, $F_\nu(\lambda) = F_o$, is assumed for standardized SNR calculation. Given its corresponding AB magnitude, $m_o = -2.5\log_{10}(F_o/3631{\rm Jy})$, the source counts in a given band b can be computed from (see eq. 6)

$$C_b = \frac{5,455}{g}10^{\,0.4(25-m_o)}\left(\frac{D}{6.5{\rm m}}\right)^2\left(\frac{\Delta t}{30\,{\rm sec}}\right)T_b, \tag{34}$$

where the only quantity dependent on the system throughput $S_b^{sys}(\lambda)$ (and independent of the source brightness) is the "throughput integral"

$$T_b = \int_0^\infty S^{atm}(\lambda)\, S_b^{sys}(\lambda)\lambda^{-1} d\lambda. \tag{35}$$

The values of T_b, computed for the standard atmosphere and a representative example of the system response, are listed in Table 2. The representative example is based on an early approximation of the expected LSST system response.

The throughput integral, T_b, is one of the two quantities required for computing SNR. The other quantity is the "system integral",

$$\Sigma_b = \int_0^\infty S_b^{sys}(\lambda)\lambda^{-1} d\lambda, \tag{36}$$

which is a measure of the system impact on the overall throughput. It can be thought of as an appropriate "average" value of the **system** throughput in a given band (i.e. no atmosphere is included), and it enters in computation of sky counts (since sky emission is not extincted by the atmosphere, eq. 40 involves Σ_b, while eq. 34 involves T_b). The values of the "system integral" computed for the baseline system response are also listed in Table 2. Note that the impact of atmospheric transmissivity on the final SNR ("effective" atmospheric extinction) in each band can be defined as

$$k_b^{atm} = -2.5 \log_{10}(T_b/\Sigma_b) \ \ \text{mag}. \tag{37}$$

For convenience, we also define two quantities that do **not** enter the SNR calculations, but may be useful during design. The "effective" wavelength for the system throughput (no atmosphere is included!) is defined as

$$\lambda^{eff} = \frac{\int_0^\infty \lambda S_b^{sys}(\lambda) d\lambda}{\int_0^\infty S_b^{sys}(\lambda) d\lambda} \tag{38}$$

and the "average" system throughput as

$$A_b^{sys} = \frac{\int_0^\infty S_b^{sys}(\lambda) d\lambda}{\Delta\lambda}, \tag{39}$$

where the "effective" filter width, $\Delta\lambda \equiv \lambda^R - \lambda^B$, is defined by points where S_b^{sys} drops to 5% of its peak value.

The standardized sky counts per pixel are computed using m_b^{sky} given by eq. 8 (and listed in Table 1), a pixel scale of 0.2 arcsec, a 30 second long integration, and $D = 6.5$m, via

$$B_b = \frac{5,455}{g} \left(\frac{D}{6.5\text{m}}\right)^2 \left(\frac{\Delta t}{30\,\text{sec}}\right) \left(\frac{\text{pixScale}}{1\,\text{arcsec}}\right)^2 10^{\,0.4(25-m_b^{sky})}\, \Sigma_b. \tag{40}$$

The resulting values of B_b are listed in Table 2 (note that the sky counts are computed using Σ_b, and not T_b).

Following eq. 28, the standardized SNR is computed as

$$SNR_b^{std} = \frac{C_b}{(C_b/g + \sigma_{tot}^2 n_{\text{eff}})^{1/2}} \tag{41}$$

where $n_{\rm eff}$ is given by eq. 31 and σ_{tot} by (assuming $\sigma_B = 0$)

$$\sigma_{tot}^2 = B_b/g + \sigma_{inst}^2. \tag{42}$$

We adopt standardized values of instrumental noise, $\sigma_{inst} = 10$ photo-electrons (not ADU!) per pixel, and gain $g = 1.0$. It is easy to show that they enter the SNR calculation from eq. 41 only as a product ($g\sigma_{inst}$), and have negligible impact on the SNR values when the background noise dominates other noise components (such as the SNR=5 case in all bands but the u band, see Section 5.2).

Table 2 also lists the corresponding AB magnitudes for sources with flat spectral energy distribution which would produce 1 ADU count/sec for an instrument with an effective aperture diameter of D, computed using eq. 34 and termed "Instrumental Zeropoint",

$$m_b^Z = 25 + 2.5\log_{10}(Z_b) \tag{43}$$

where

$$Z_b = \frac{181.8}{g}\left(\frac{D}{6.5{\rm m}}\right)^2 T_b. \tag{44}$$

It is straightforward to compute counts corresponding to detections of unresolved sources at an arbitrary[4] SNR from (by solving eq. 41)

$$C_b(SNR) = \frac{(SNR)^2}{2g} + \left(\frac{(SNR)^4}{4g} + (SNR)^2\, V_N\right)^{1/2}, \tag{45}$$

where (see eqs. 31 and 42)

$$V_N = 2.436\,({\rm FWHM/pixelScale})^2(B_b/g + \sigma_{inst}^2). \tag{46}$$

With $C_b(SNR)$, and given m_b^Z, the corresponding magnitude can then be computed from

$$m_b(SNR) = m_b^Z + 2.5\log_{10}\left(\frac{\Delta t}{1\,{\rm sec}}\right) - 2.5\log_{10}\left[C_b(SNR)\right]. \tag{47}$$

The baseline values of these magnitudes computed for SNR=5 are also listed in Table 2 (row 11) and are compared to the corresponding SRD requirements (rows 12 and 13).

As evident, the representative example of system throughput used in computations exceeds the SRD specifications by a comfortable margin in all bands (rows 14 and 15). **However, this is only an illustration based on estimated throughput functions! For generalized constraints on the system throughput based on the SRD single-visit depth requirements see the next Section (§ 6)**

[4]Note that various systematics associated with very bright sources are not discussed in this document.

Row	Quantity	u	g	r	i	z	y_2	y_3	y_4
1	m_b^{sky} (AB)	22.92	22.27	21.20	20.47	19.59	18.46	18.42	18.63
2	T_b	0.0379	0.1493	0.1386	0.1198	0.0838	0.0123	0.0193	0.0413
3	Σ_b	0.0574	0.1735	0.1502	0.1272	0.0872	0.0127	0.0199	0.0469
4	Seeing	0.77	0.73	0.70	0.67	0.65	0.63	0.63	0.63
5	A_b^{sys}	0.262	0.490	0.565	0.583	0.531	0.186	0.172	0.262
6	λ_b^{eff} (nm)	365.49	480.03	622.20	754.06	868.21	991.66	1004.90	973.37
7	k_b^{atm}	0.451	0.163	0.087	0.065	0.043	0.035	0.033	0.138
8	Sky B_b	85.07	467.9	1085.2	1800.3	2775.7	1144.6	1860.8	3614.3
9	Source Counts	421.4	691.4	952.9	1152	1373	879.8	1101	1511
10	m_b^Z	27.09	28.58	28.50	28.34	27.95	25.87	26.36	27.18
11	m_b^{stnd} (AB)	24.22	25.17	24.74	24.38	23.80	22.20	22.45	22.93
12	m_5^{SRD} (v4.3)	23.9	25.0	24.7	24.0	23.3	22.1	22.1	22.1
13	$m_5^{stnd} - m_5^{SRD}$	0.32	0.17	0.04	0.38	0.50	0.10	0.35	0.83
14	SNR(m_5^{SRD})	6.69	5.87	5.23	7.09	7.93	5.50	6.88	10.68
15	T_b^{SRD}/T_b	0.69	0.76	0.92	0.52	0.42	0.84	0.55	0.24

Table 2: The Standardized SNR Calculation. The first four rows list the necessary input: the dark sky brightness (AB mag/arcsec^2), the throughput integral T_b (see eq. 35) and the system integral Σ_b (see eq. 36), and adopted seeing (FWHM in arcsec) for each band. The next three rows list "convenience" quantities: the fifth row lists the "average" system throughput in each band, as defined by eq. 39), the sixth row lists the "effective" wavelength (see eq. 38), and the seventh row lists the "effective" atmospheric extinction (see eq. 37). Rows 8-11 lists sky counts per pixel (eq. 40), source counts (eq. 34), the "instrumental zeropoint" (eq. 43), and the magnitude corresponding to SNR=5 (eq. 41). The corresponding limiting magnitudes from the SRD (m_5^{SRD}) are listed in row 12. Row 13 lists the differences between rows 11 and 12, and row 14 lists the SNR for source whose brightness is equal to m_5^{SRD}. A factor by which baseline T_b and Σ_b should be multiplied to achieve m_5^{SRD} with the baseline throughput is listed in the last row.

5.1. Summary of Standard SNR Calculations

In order to compute SNR for a given source, or at what source brightness certain SNR would be achieved, the following input parameters are required:

1. Source flux normalization, F_o, or the corresponding magnitude, m_o. An alternative is to fix SNR and compute source brightness. *Standardized computations assume a source with flat spectral energy distribution (F_ν).*

2. Atmospheric transmissivity described by $S^{atm}(\lambda)$. *Standardized computations are based on a fixed input function available from Document-8817.*

3. Sky brightness (emission spectrum) described by $b_\nu^{sky}(\lambda)$ (see Section 3). *Standardized computations are based on a fixed input function available from Document-8818.*

4. System throughput described by $S_b^{sys}(\lambda)$. This function is a result of the system design process and represents the main "interface" between a given system design and the SRD requirements for SNR. The current baseline is available as consecutively numbered files from Document-8846 to Document-8853, in Collection-1777.

5. Instrumental noise, σ_{inst}, is set to a *fiducial* value of 10 photo-electron/pixel/visit. This fiducial value is motivated by two readouts with a readout noise of 5 photo-electron/pixel/readout and the rest is due to dark current noise and any other noise source. *These parameters have only a second-order impact on the resulting SNR* (and have a higher impact in the u band, see Section 5.2 below).

5.2. A Comment on the Impact of Instrumental Noise on Limiting Depth in the u Band

The dominant noise contribution at SNR=5 is the sky in all bands except the u band (see Table 3). With adopted instrumental noise of $\sigma_{inst} = 10$ photo-electrons per pixel, the noise from the sky and the instrument are comparable in the u band. If the instrumental noise could be decreased by a factor of 2 (e.g. readout noise of 3 photo-electrons per pixel, with small dark current noise), the limiting depth in the u band would improve by 0.26 mag. With the baseline allocation of 5% of the observing time to the u band, this difference is equivalent to 0.3 years of survey time.

Row	Quantity	u	g	r	i	z	y_2	y_3	y_4
1	Sky noise	55.42	123.2	180.0	221.8	267.2	166.3	212.1	295.6
2	Instrument noise	60.09	57.0	54.6	52.3	50.7	49.2	49.2	49.2
3	Source Noise	20.53	26.3	30.9	33.9	37.0	29.7	33.2	38.9

Table 3: The total noise contribution from the sky, instrument and source, in counts, for a source detection corresponding to row 11 in Table 2 (with $n_{\rm eff} = 36.11$ pixels, see eq. 31). For example, when all three noise contributions in the u band are added in quadrature, they produce a total noise of 84.3 counts. This noise level corresponds to an SNR=5 detection of a source with 421.4 counts (see row 9 in Table 2). Note that the instrument noise is larger than the sky noise in the u band for the assumed $\sigma_{inst} = 10$ photo-electrons per pixel.

6. Standardized Generalized Constraints on the System Throughput

The analysis in Section 5 was based on a representative but only illustrative example of the system throughput function. If the *shape* of the system throughput function could be assumed unchangeable, the results from Table 2 could be rescaled to predict SNR for any other normalization (as was done in the last row in Table 2). However, the variations in existing sensor QE for different vendors make this assumption invalid. To generalize the standardized SNR calculation to an arbitrary system throughput function, a piecewise linear approximation within the wavelength

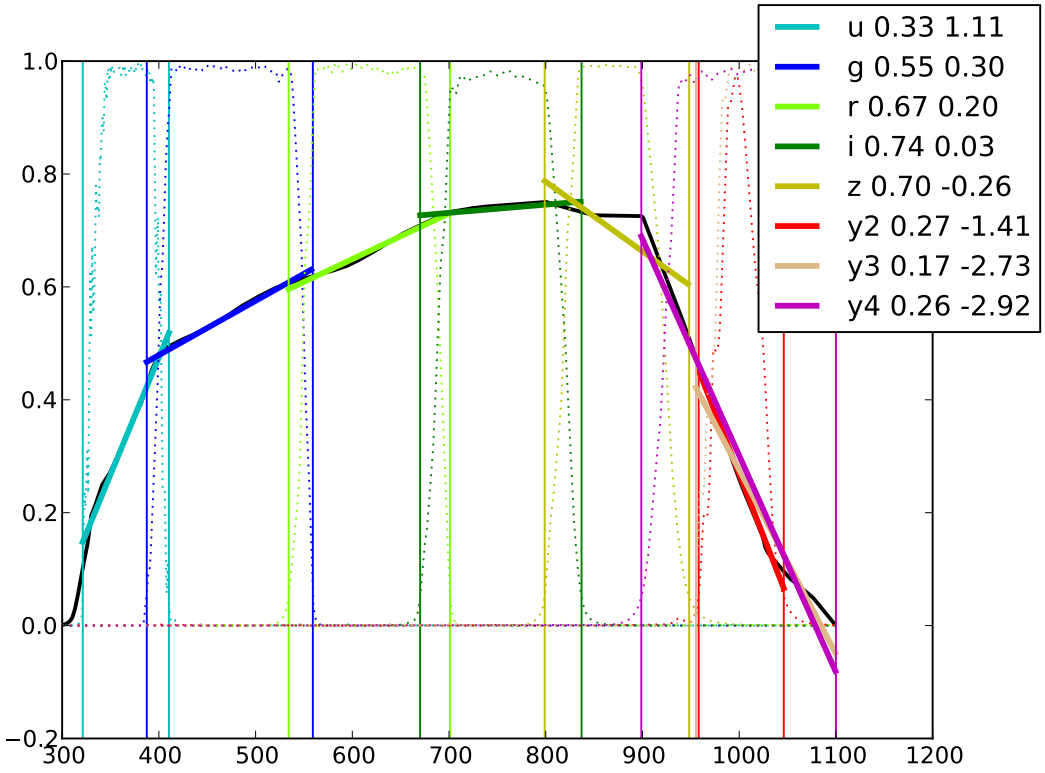

Fig. 5.— An example of piecewise linear fits to the system throughput that includes mirrors, lenses and the sensor quantum efficiency (but not the filters). The throughput is shown by the black line, and the filters are shown by dotted lines. The piecewise linear fits within wavelength ranges marked by the vertical lines are shown by thick colored lines. The inset shows the best-fit parameters S_o and β_o (see eq. 48).

boundaries of each filter bandpass suffices at the accuracy level of 1-2% (of the resulting throughput normalization - not in an absolute sense). We adopt nomenclature

$$S^{\rm hw}(\lambda) = S_o \left(1 + \beta(\frac{\lambda - \lambda^{eff}}{\lambda^R - \lambda^B})\right) \tag{48}$$

where the "hardware" throughput (without filters!) is defined as

$$S^{\rm hw}(\lambda) \equiv S^{\rm mirrors}(\lambda)\, S^{\rm lenses}(\lambda)\, S^{\rm detector}(\lambda), \tag{49}$$

and parameters β, λ^{eff}, λ^R and λ^B are defined for each filter separately (for the latter three, see eqs. 38 and 39). Figure 5 illustrates these approximations for the throughput functions used in previous section (note that the best-fit linear approximation to the y band throughput becomes negative close to the red edge).

Informed by the best-fit β values from Figure 5, we chose reference values for each band, β_o, listed in Table 4. It turns out that corrections for different β values (proportional to the slope of the piecewise linear approximations) are not large (they are akin to astronomical "color terms") and the following expression can be used to compute the SRD-driven constraints on the system throughput for any plausible value of β

$$S_o^{SRD}(\beta) = S_o^{SRD}(\beta = \beta_o) + \sigma_\beta \, (\beta - \beta_o) \, , \tag{50}$$

where σ_β are listed in Table 4. The accuracy of this approximation is 1-2% of the true $S_o^{SRD}(\beta)$ value (i.e., $< 1\%$ of the total throughput). In particular, should one wish to adopt $\beta = 0$ for all bands, the S_o^{SRD} values for the u band and the y_4 band would both increase by 0.004 (a change of 2% and 6% of the listed $S_o^{SRD}(\beta_o)$ values, respectively).

The listed values of S_o^{SRD} approximately correspond to the fraction of captured photons that hit the telescope pupil, and give constraints on the system throughput losses due to mirrors, lenses and detectors (but not filters!). The corresponding values of the throughput integral T_b (see eq. 35) and the system integral Σ_b (see eq. 36) **represent generalized SRD-based constraints on the system throughput,** and are listed in the last two rows in Table 4. To summarize, these results are based on the atmospheric transmissivity function listed in Document-8817, the dark sky spectrum listed in Document-8818, and the filter curves listed in consecutively numbered files from Document-8820 to Document-8827, all available from Collection-1777. No other wavelength-dependent functions are required to reproduce the results from Table 4.

Row	Quantity	u	g	r	i	z	y$_2$	y$_3$	y$_4$
1	λ_b^{eff} (nm)	365.49	480.03	622.20	754.06	868.21	991.66	1004.90	973.37
2	λ_b^B (nm)	318.5	388.6	534.9	670.1	798.7	958.1	954.9	895.4
3	λ_b^R (nm)	405.2	559.4	701.2	837.1	942.5	1046.1	1090.0	1088.8
4	$S_o^{SRD}(\beta_o)$	0.217	0.440	0.626	0.392	0.308	0.210	0.091	0.064
5	β_o	1.0	0.0	0.0	0.0	0.0	-2.0	-2.0	-2.0
6	m_b^{sky} (AB)	22.90	22.29	21.21	20.48	19.57	18.53	18.39	18.56
7	σ_β	-0.004	0.016	0.038	0.023	0.024	0.007	0.003	0.002
8	F^{eff}	0.785	0.863	0.837	0.774	0.710	0.539	0.841	0.872
9	T_b^{SRD}	0.0263	0.1153	0.1289	0.0627	0.0357	0.00986	0.0108	0.0102
10	Σ_b^{SRD}	0.0411	0.1387	0.1420	0.0674	0.0376	0.01028	0.0110	0.0115

Table 4: The standardized SNR calculation for a generalized system response given by eq. 48. The first three rows list the fiducial wavelengths: the effective wavelength (see eq. 38), and the blue and red wavelength boundaries (where the filter transmission functions drop to 5% of their maximum values). The fourth row lists the value of S_o parameter from eq. 48 that corresponds to the single-visit depths listed in the SRD. This value is computed for the fiducial value of parameter β listed in row 5, and is based on the sky brightness listed in row 6 (the listed sky brightness is slightly different from the values listed in row 1 from Table 1 due to the use of linear approximation for the system throughput). The derivative of S_o with respect to β (see eq. 50) is listed in row 7. For completeness, the impact of filter transmission, computed using eq. 39 with $S_b^{sys}(\lambda)$ replaced by $S^{\rm filter}(\lambda)$, are listed in row 8. The values of the throughput integral T_b (see eq. 35) and the system integral Σ_b (see eq. 36) that correspond to S_o listed in row 4 are listed in the last two rows.

Appendix A: The Impact of optics, detectors and atmosphere on total throughput

For completeness, the impact of optics, detectors and atmosphere on total throughput is illustrated in Fig. 6. Note that the blue edge of the u band is affected by both optics and atmosphere, while the red edge of the y bands is controlled by the detector quantum efficiency.

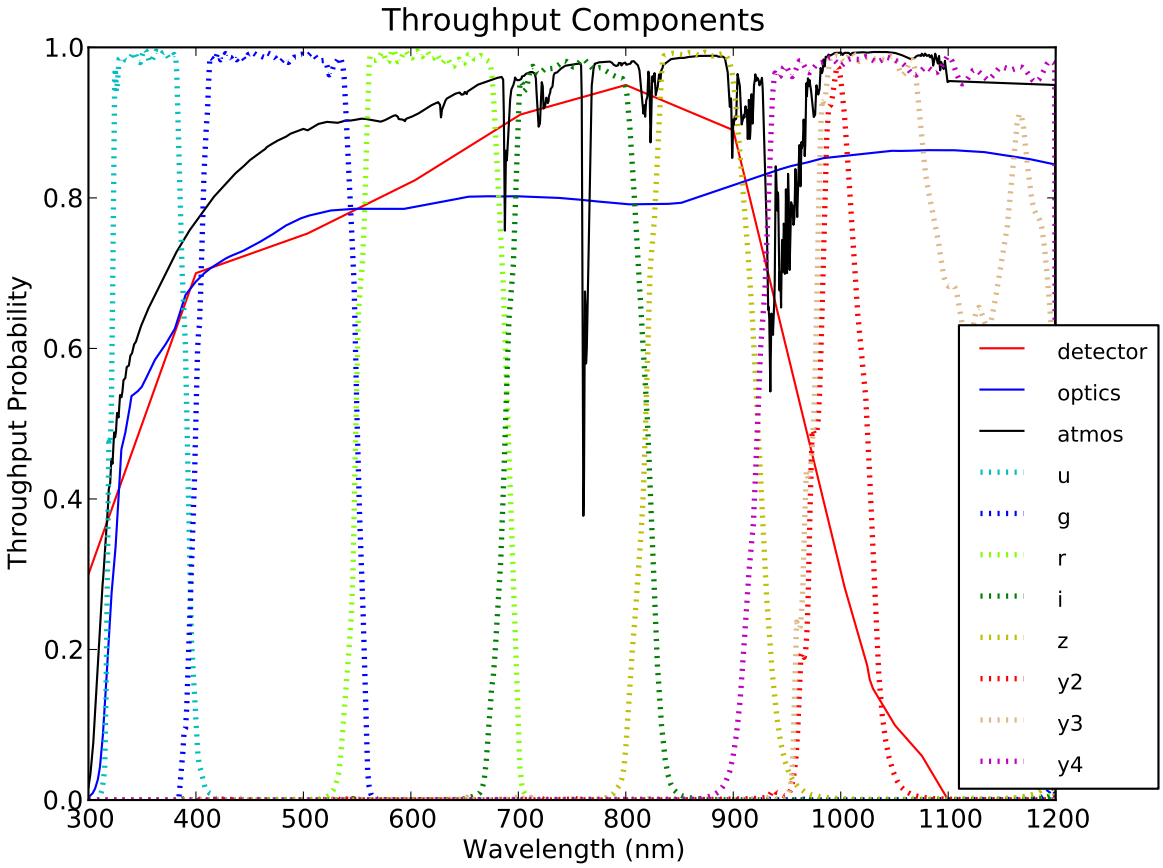

Fig. 6.— The atmospheric transmissivity is shown by the black line, the optics transmission (lenses and mirrors, but without filters) is shown by the blue line, and the adopted detector quantum efficiency is shown by the red line. The filter curve for each band is shown by colored lines, according to the legend.

Appendix B: Different y Band Options

The three y band options are illustrated in Fig. 7. The current baseline is the y_3 filter, and y_4 is being considered as the new baseline.

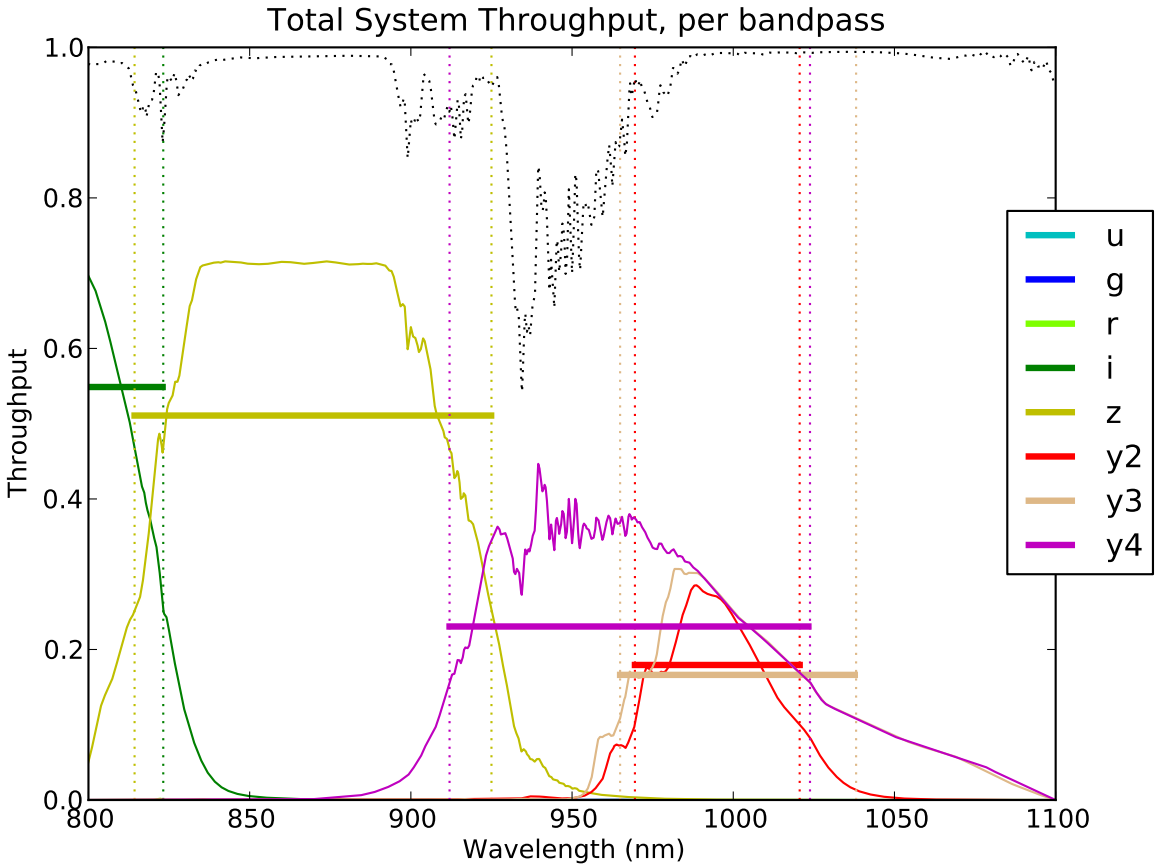

Fig. 7.— The adopted total throughput for the z band and the three y bands. The black dotted line shows the atmospheric transmissivity and the vertical lines show wavelengths where the system throughput function (for the baseline values) drops to 5% of the maximum value in each band.

Appendix C: Python Code for Performing the Standardized SNR Calculations

The python script 'thruputLite.py' is available from Docushare Collection-1777 (AA-thruputLite* files, and in particular Document-8843, which contains how-to comments). This code provides an easy-to-use tool for performing calculation of the 5σ limiting magnitude for any combination of detector + optics (lenses and mirrors) + filter throughput files. It uses a standardized dark sky SED and atmosphere throughput file (also available in Collection-1777). For the input values of the readnoise, darkcurrent and throughputs that are standardized and available from Collection-1777, the code you will reproduce results listed in tables from this document.

Usage is as follows: *>python thruputLite.py thruputLite.input.*

Users can study the effect on the 5σ point source limiting magnitude of different throughput files by changing the name of the files used to build the total throughput, via the 'thruputLite.input' file. This input file specifies the names of each component (such as the filter, each individual mirror,

each individual lens, and the detector) used to compile the total throughput. The dark sky SED and the atmosphere throughput files are specified here as well, along with exposure time, the diameter of the primary mirror, the expected seeing value, etc. (these are not expected to be changed by most users). In addition to calculating the system values of the 5σ limiting magnitude, total throughput, etc., the program will calculate the SNR and noise sources for the system, for a user-specified magnitude specified as 'mag' in the thruputLite.input file.

Output of the program will look like (this is an example for the u band):

```
> python thruputLite.py thruputLite.input

Using user input file /Users/ljones/work/code/lsstpython/thruputLite.input
Telescope throughput parameters:
System throughput integral (system only, no atmosphere): 0.057151
Total throughput integral (system + atmosphere): 0.037752
Effective wavelength (nm) 365.492351
Instrumental zeropoint for this bandpass: 27.091500
Sky magnitude (mag/'') and electrons (e-/pix): 22.916109  84.999875
Five-Sigma limiting magnitude (AB) for this bandpass: 24.222732

Now calculating SNR and relevant values for the user-requested source
    at 24.322000 magnitudes
For Nexp 2.0 of time 15.0:
Counts from source: 384.52  Counts from sky: 85.00
Noise from sky: 9.22   Noise from instrument: 10.00  Neff: 36.108(pix)
Noise from source: 19.61
Total Signal: 384.52   Total Noise: 84.05    SNR: 4.58
```